

# A differential quadrature analysis of vibration and buckling of an SS-C-SS-C rectangular plate loaded by linearly varying in-plane stresses

Xinwei Wang\*, Lifei Gan, Yongliang Wang

*College of Aerospace Engineering, Nanjing University of Aeronautics & Astronautics, Nanjing 210016, China*

Received 24 August 2005; received in revised form 29 March 2006; accepted 5 June 2006

Available online 28 July 2006

---

## Abstract

Thin rectangular plates having two opposite edges simply supported, with those edges subjected to linearly varying in-plane stresses, and the other two edges clamped, are encountered in engineering practice. Recently, Leissa and Kang used the classical power series method and obtained the first known exact vibration and some buckling solutions. The classical plate theory based on the Kirchhoff hypothesis is employed in the analysis. The relatively wild character of the convergence is observed, however, and 20 or 30 more terms of the series are needed to obtain reasonably accurate results. The differential quadrature (DQ) method has proved an accurate and computationally efficient numerical method. Thus, the DQ method is used to study the vibration and buckling of an SS-C-SS-C rectangular plate loaded by linearly varying in-plane stresses. Convergence study shows that DQ method with  $15 \times 15$  or more non-uniform grid points can yield very accurate results for cases considered. Exactly the same, accurate results as of Leissa and Kang are easy to reproduce.

© 2006 Elsevier Ltd. All rights reserved.

---

## 1. Introduction

The transverse free vibrations and buckling of plates subjected to edge compressive loadings is an area of research that had received a great deal of attention in the last century [1,2]. Obtaining exact solutions is straightforward when two opposite edges of rectangular plates are simply supported and subjected to uniform loadings. However, a plate may be loaded at two opposite edges by non-uniform in-plane loadings. The first variation from the uniform loading is one which varies linearly, for example, a pure in-plane bending moment. The second variation from the uniform loading varies parabolically or as a half-sine wave. Due to the mathematical complexity, there have been only a few works on the case of non-uniformly distributed edge loadings.

Recently, Leissa and Kang [3] employed the power-series methods to give the first known exact solutions for free vibration and buckling of a loaded SS-C-SS-C rectangular thin plate. The plate considered to be simply supported at two opposite edges and the loadings were varying linearly in-plane. The other two edges were

---

\*Corresponding author.

E-mail address: [wangx@nuaa.edu.cn](mailto:wangx@nuaa.edu.cn) (X. Wang).

taken clamped. The classical plate theory based on the Kirchhoff hypothesis is used. Although, only one in-plane stress component inside the plate with the same distribution as the applied edge loading needs to be considered, the convergence has the relatively wild character. Convergence is not monotonic but oscillatory and the oscillation amplitude does not necessarily decrease as more terms are added. Analysis makes these clear. Thus, 30 terms, why even 120 terms of the series are needed to obtain accurate solutions. Bert and Devarakonda [4] used Galerkin method to obtain more accurate buckling loads of a loaded rectangular thin plate when all edges are simply supported (SS-SS-SS-SS plate) and subjected to nonlinearly varying edge loads. They found the problem much complicated compared to the case with linearly varying in-plane loadings since all the three in-plane stress components inside the plate need to be considered during buckling analysis. Hence, one gets only approximate solutions [4]. If the plate is not thin or if the transverse shear deformation is not negligible, shear deformation theories must be employed. In such cases, it is even harder to obtain closed-form solutions, and numerical schemes such as the finite element method and finite difference method have to be resorted too. Various finite elements have been developed recently to investigate, for example, the buckling and vibration analysis of initially stressed damped composite sandwich plates [5], the buckling and vibration analysis of initially stressed composite sandwich plates [6], and dynamic stability of doubly curved panels with and without cutout subject to non-uniform harmonic loadings [7,8].

The differential quadrature (DQ) method is a numerical technique for initial- or/and boundary-value problems originated by Bellman and Casti [9]. This method is based on the approximation of a function and hence its partial derivatives with respect to the space variables, within a domain, by a linear sum of function values at all discrete grid points. Bert et al. [10] are the first ones to use DQ method for solving problems in structural mechanics. Since then, DQ method has been successfully used for solutions of static, free vibration and buckling of thin and moderately thick plates [11,12]. It has been shown by many researchers that DQ method is accurate and computationally efficient, thus is projected as a potential alternative to the conventional numerical methods such as finite element and finite difference methods. Additional details on the developments of the DQ method and on its applications may be found, for example, in Refs. [13–15].

Analysis of the transverse free vibrations and buckling of plates subjected to edge-compressive non-uniformly distributed loadings with the use of DQ method is not attempted so far to the best of the authors' knowledge. Hence, the focus of this paper is to extend the DQ method for studying the free vibration and buckling solutions of rectangular plates subjected to linearly varying in-plane stresses. The classical plate theory based on the Kirchhoff hypothesis is used in the analysis. To make the DQ method even simpler and more accurate for obtaining frequency and buckling loads, built-in methods proposed by the senior author recently [16,17], are used for applying the boundary conditions. Detailed formulations are given and convergence study is performed to determine the number of grid points. To demonstrate that the DQ method could provide the benchmark for the development of other numerical techniques, numerical results are given and compared with available exact solutions.

## 2. Mathematical equations

Consider an isotropic rectangular plate with dimensions of  $a \times b$ , as shown in Fig. 1. The plate that is simply supported (SS) at  $x = \pm a/2$  is taken to be under linearly varying in-plane stresses at these two edges. The other two edges ( $y = \pm b/2$ ) are clamped (C). In other words, an SS-C-SS-C rectangular plate is considered.

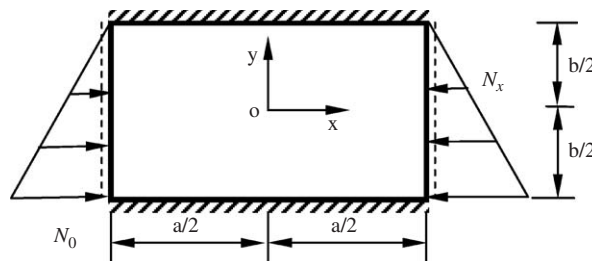


Fig. 1. An SS-C-SS-C rectangular plate under compressive load ( $\alpha = 1$ ).

The differential equation of motion governing vibration and buckling is

$$D \left( \frac{\partial^4 \bar{w}}{\partial x^4} + 2 \frac{\partial^4 \bar{w}}{\partial x^2 \partial y^2} + \frac{\partial^4 \bar{w}}{\partial y^4} \right) + \rho h \frac{\partial^2 \bar{w}}{\partial t^2} = q + N_x \frac{\partial^2 \bar{w}}{\partial x^2} + 2N_{xy} \frac{\partial^2 \bar{w}}{\partial x \partial y} + N_y \frac{\partial^2 \bar{w}}{\partial y^2}, \tag{1}$$

where  $\bar{w}(x, y, t)$  is the transverse displacement,  $\rho$  is the mass density per unit volume,  $h$  is the plate thickness,  $q$  is a distributed load per unit surface area applied to the lateral surface,  $D$  is the flexural rigidity of the plate,  $N_{xy}$  is shearing force per unit length in the  $xy$ -plane,  $N_x$  and  $N_y$  are normal forces per unit length of plate in the  $x$  and  $y$  directions, respectively.

Denote by  $E$  and  $\nu$  Yang’s modulus and Poisson’s ratio, respectively and by  $\sigma_x, \sigma_y, \tau_{xy}$  the normal stresses in  $x$ -,  $y$ -direction, and the shear stress in the  $xy$ -plane, respectively. Then, one has

$$D = \frac{Eh^3}{12(1 - \nu^2)}, \tag{2}$$

$$N_x = \sigma_x h, \quad N_y = \sigma_y h, \quad N_{xy} = \tau_{xy} h. \tag{3}$$

Assume  $q = N_y = N_{xy} = 0$  and consider the linearly varying compressive load in the  $x$ -direction defined by

$$N_x = -N_0 \left[ 1 - \alpha \left( \frac{y}{b} + \frac{1}{2} \right) \right], \quad y \in \left[ -\frac{b}{2}, \frac{b}{2} \right]. \tag{4}$$

Then, Eq. (1) simplifies to

$$D \left( \frac{\partial^4 \bar{w}}{\partial x^4} + 2 \frac{\partial^4 \bar{w}}{\partial x^2 \partial y^2} + \frac{\partial^4 \bar{w}}{\partial y^4} \right) + \rho h \frac{\partial^2 \bar{w}}{\partial t^2} = -N_0 \left[ 1 - \alpha \left( \frac{y}{b} + \frac{1}{2} \right) \right] \frac{\partial^2 \bar{w}}{\partial x^2}. \tag{5}$$

Furthermore, assume

$$\bar{w}(x, y, t) = w(x, y) \sin(\omega t), \tag{6}$$

where  $\omega$  is the circular frequency. Then, Eq. (5) is reduces to

$$D \left( \frac{\partial^4 w}{\partial x^4} + 2 \frac{\partial^4 w}{\partial x^2 \partial y^2} + \frac{\partial^4 w}{\partial y^4} \right) - \rho h \omega^2 w = -N_0 \left[ 1 - \alpha \left( \frac{y}{b} + \frac{1}{2} \right) \right] \frac{\partial^2 w}{\partial x^2}. \tag{7}$$

Define the non-dimensional frequency ( $\lambda$ ) and non-dimensional load ( $N^*$ ) at  $x = \pm a/2$  by

$$\lambda = \omega a^2 \sqrt{\frac{\rho h}{D}}, \quad N^* = \frac{N_0 b^2}{D}. \tag{8}$$

The boundary conditions to be considered are:

1. Simply supported (SS) at  $x = -a/2, a/2$ :  $w = M_x = 0$  or  $w = w_{xx} = 0$ ,
2. Clamped (C) at  $y = -b/2, b/2$ :  $w = w_y = 0$ ,

where

$$w_{xx} = \frac{\partial^2 w}{\partial x^2}, \quad w_y = \frac{\partial w}{\partial y}.$$

Eq. (7) is to be solved by using the DQ method. In terms of differential quadrature, the governing differential equation at inner grid point are expressed by

$$\sum_{k=2}^{n_x-1} D_{ik}^x w_{kl} + 2 \sum_{j=2}^{n_x-1} \sum_{k=2}^{n_y-1} B_{ij}^x B_{lk}^y w_{jk} + \sum_{k=2}^{n_y-1} D_{lk}^y w_{ik} - \frac{\lambda^2}{a^2} w_{il} = -\frac{N^*}{b^2} \left( \sum_{k=2}^{n_x-1} B_{ik}^x w_{kl} \left[ 1 - \alpha \left( \frac{y_{il}}{b} + \frac{1}{2} \right) \right] \right) \tag{8'}$$

( $i = 2, 3, \dots, n_x - 1; \quad l = 2, 3, \dots, n_y - 1$ )

where  $D_{ij}^x, D_{ij}^y, B_{ij}^x, B_{ij}^y$  are the weighting coefficients of the fourth-order derivatives with respect to  $x$  and  $y$ , the weighting coefficients of the second-order derivatives with respect to  $x$  and  $y$ , respectively,  $w_{il}$  and  $y_{il}$  are values of deflection and  $y$  coordinate at grid point  $il$ , respectively, and  $n_x, n_y$  are the number of grid points in the  $x$ - and  $y$ -direction, respectively. In writing Eq. (8'), the zero deflection at all boundary points has been taken into consideration.

The other boundary condition is to be built in while formulating the weighting coefficients of higher order derivatives. Built-in method (1) is to be used for the simply supported boundary condition [16,17]. Built-in method (4) is to be used for the clamped boundary condition [17]. Previous experience showed that  $n_x = n_y = N$  gave the best convergence rate. Thus, the number of grid points in both directions is taken the same as  $N$ .

Denote  $A_{ij}^x$  and  $A_{ij}^y$  the weighting coefficients of the first-order derivatives with respect to  $x$  and  $y$ , respectively. They can be computed explicitly by [15]

$$A_{ij}^x = \frac{\omega'_N(x_i)}{(x_i - x_j)\omega'_N(x_j)} \quad (i \neq j), \quad A_{ii}^x = \sum_{j=1, i \neq j}^N \frac{1}{(x_i - x_j)}, \tag{9}$$

$$A_{ij}^y = \frac{\omega'_N(y_i)}{(y_i - y_j)\omega'_N(y_j)} \quad (i \neq j), \quad A_{ii}^y = \sum_{j=1, i \neq j}^N \frac{1}{(y_i - y_j)}, \tag{10}$$

where

$$\omega_N(x) = (x - x_1)(x - x_2) \dots (x - x_{i-1})(x - x_i)(x - x_{i+1}) \dots (x - x_N), \tag{11a}$$

$$\omega'_N(x) = (x - x_1)(x - x_2) \dots (x - x_{i-1})(x - x_{i+1}) \dots (x - x_N), \tag{11b}$$

$$\omega_N(y) = (y - y_1)(y - y_2) \dots (y - y_{i-1})(y - y_i)(y - y_{i+1}) \dots (y - y_N), \tag{12a}$$

$$\omega'_N(y) = (y - y_1)(y - y_2) \dots (y - y_{i-1})(y - y_{i+1}) \dots (y - y_N). \tag{12b}$$

To build in the second boundary condition at  $x = \pm a/2$ , namely,  $(w_{xx})_1 = (w_{xx})_N = 0$ , the weighting coefficients of the fourth-order derivatives with respect to  $x$ ,  $D_{ij}^x$ , is computed by

$$D_{ij}^x = \sum_{k=2}^{N-1} B_{ik}^x B_{kj}^x \quad (i, j = 1, 2, \dots, N), \tag{13}$$

where  $B_{ij}^x$  are the weighting coefficients of the second-order derivatives with respect to  $x$ , computed by

$$B_{ij}^x = \sum_{k=1}^N A_{ik}^x A_{kj}^x \quad (i, j = 1, 2, \dots, N). \tag{14}$$

To build in the second boundary condition at  $y = \pm b/2$ , namely,  $(w_y)_1 = (w_y)_N = 0$ , the weighting coefficients of the second-order derivatives with respect to  $y$ ,  $B_{ij}^y$ , is computed by

$$B_{ij}^y = \sum_{k=2}^N A_{ik}^y A_{kj}^y \quad (i = 1, 2, \dots, N_h, j = 1, 2, \dots, N), \tag{15}$$

$$B_{ij}^y = \sum_{k=1}^{N-1} A_{ik}^y A_{kj}^y \quad (i = N_h + 1, N_h + 2, \dots, N, j = 1, 2, \dots, N), \tag{16}$$

where  $N_h = N \div 2$  and  $N$  is an even number. If  $N$  is an odd number, Eq. (16) is replaced by the following two equations:

$$B_{ij}^y = \sum_{k=1}^N A_{ik}^y A_{kj}^y \quad (i = N_h + 1, j = 1, 2, \dots, N), \tag{17}$$

$$B_{ij}^y = \sum_{k=1}^{N-1} A_{ik}^y A_{kj}^y \quad (i = N_h + 2, N_h + 3, \dots, N, \quad j = 1, 2, \dots, N). \tag{18}$$

The weighting coefficients of the fourth-order derivatives with respect to  $y$ ,  $D_{ij}^y$ , is computed by

$$D_{ij}^x = \sum_{k=1}^N \bar{B}_{ik}^y B_{kj}^y \quad (i, j = 1, 2, \dots, N), \tag{19}$$

where  $\bar{B}_{ij}^y$  are computed by

$$\bar{B}_{ij}^y = \sum_{k=1}^N A_{ik}^y A_{kj}^y \quad (i, j = 1, 2, \dots, N). \tag{20}$$

Note that the summation ranges in Eqs. (13), (15), (16) and (18) are slightly different from 1 to  $N$  to build in the other zero boundary condition.

In the DQ analysis, the following non-uniform grid spacing is used since the problem is sensitive to grid spacing:

$$\begin{aligned} x_i &= -a \cos[(i - 1)\pi/(N - 1)]/2, \\ y_i &= -b \cos[(i - 1)\pi/(N - 1)]/2, \quad i = 1, 2, \dots, N. \end{aligned} \tag{21}$$

Eq. (8') can be written in the matrix form as follows:

$$[K]\{w\} - \frac{\lambda^2}{a^2}[I]\{w\} + \frac{N^*}{b^2}[K_\sigma]\{w\} = \{0\}, \tag{22}$$

where the size of the matrices is  $(N - 2)^2 \times (N - 2)^2$ . Solving the generalized eigenvalue problem, Eq. (22), yields the buckling load (the lowest eigen-value) and frequencies.

### 3. Convergence study

Consider first the free vibration of an unloaded SS-C-SS-C square plate. In the analysis, the material constants are:  $E = 206.0$  Gpa and  $\rho = 7900$  kg/m<sup>3</sup>; the dimensions are:  $a = 1.0$  m,  $h = 0.005$  m, and  $b$  is computed according to the aspect ratios. Actually the non-dimensional results listed in Tables 1–9 are

Table 1  
Convergence of non-dimensional frequencies  $\lambda = \omega a^2 \sqrt{\rho h/D}$  of an unloaded SS-C-SS-C square plate ( $a/b = 1$ ) for  $m = 1$

$N$	1	2	3	4	5
9	28.9493	69.1179	—	—	—
10	28.9510	69.3467	—	—	—
11	28.9509	69.3270	129.494	—	—
12	28.9508	69.3266	129.078	—	—
13	<b>28.9509</b>	69.3268	129.100	208.357	—
14	28.9509	<b>69.3270</b>	129.092	208.337	307.037
15	28.9509	69.3270	129.096	208.370	307.366
16	28.9509	69.3270	129.095	208.395	307.196
17	28.9509	69.3270	<b>129.096</b>	<b>208.392</b>	307.360
18	28.9509	69.3270	129.096	208.392	307.314
19	28.9509	69.3270	129.096	208.392	307.317
20	28.9509	69.3270	129.096	208.392	<b>307.316</b>
21	28.9509	69.3270	129.096	208.392	307.316
22	28.9509	69.3270	129.096	208.392	307.316
23	28.9509	69.3270	129.096	208.392	307.316
Leissa [3]	28.95(22)	69.33(29)	129.1(36)	208.4(44)	307.766(50)
Exact	28.9509	69.3270	129.096	208.392	307.316

Table 2  
Convergence of non-dimensional critical buckling loads  $N_{cr}^* = N_{cr}b^2/D$

N	$\alpha = 0$			$\alpha = 1$			$\alpha = 2$		
	a/b			a/b			a/b		
	0.4	0.5	0.7	0.5	0.6	0.7	0.5	0.7	0.75
9	92.9493	75.7851	69.0600	144.808	134.534	134.440	388.783	421.451	408.030
10	93.2863	75.9253	69.0992	<b>145.238</b>	<b>134.778</b>	<b>134.601</b>	390.736	420.828	408.037
11	93.2596	<b>75.9136</b>	69.0959	145.212	134.761	134.590	391.558	422.366	409.428
12	93.2431	75.9087	69.0947	145.203	134.759	134.589	<b>391.526</b>	422.315	409.366
13	<b>93.2463</b>	75.9097	<b>69.0952</b>	145.205	134.759	134.589	391.554	<b>422.456</b>	<b>409.472</b>
14	93.2473	75.9100	69.0952	145.206	134.759	134.589	391.545	422.464	409.473
15	93.2472	75.9099	69.0952	145.205	134.759	134.589	391.546	422.465	409.473
16	93.2472	75.9099	69.0952	145.205	134.759	134.589	391.546	422.465	409.473
17	93.2472	75.9099	69.0952	145.205	134.759	134.589	391.546	422.465	409.473
Leissa [3]	93.25 (38)	75.91 (31)	69.10 (28)	145.2 (37)	134.8 (34)	134.6 (31)	391.5 (44)	422.5 (52)	409.5 (52)

Table 3  
Convergence of non-dimensional frequencies  $\lambda = \omega a^2 \sqrt{\rho h/D}$  for  $a/b = 1$  and  $m = 2$ , and  $N_0/N_{cr} = 0.5$

N	$\alpha = 0$			$\alpha = 1$			$\alpha = 2$		
	1 2 3			1 2 3			1 2 3		
	1	2	3	1	2	3	1	2	3
9	38.65	85.98	149.7	39.05	86.46	150.0	45.72	96.58	154.4
10	38.72	86.29	148.5	39.13	86.76	148.7	45.97	96.47	154.1
11	<b>38.71</b>	<b>86.30</b>	150.2	39.13	<b>86.77</b>	150.5	<b>45.98</b>	96.62	155.7
12	38.71	86.30	149.8	39.12	86.77	<b>150.1</b>	45.98	<b>96.61</b>	<b>155.5</b>
13	38.71	86.30	<b>149.9</b>	39.12	86.77	150.1	45.98	96.61	155.5
14	38.71	86.30	149.9	<b>39.13</b>	86.77	150.1	45.98	96.61	155.5
15	38.71	86.30	149.9	39.13	86.77	150.1	45.98	96.61	155.5
16	38.71	86.30	149.9	39.13	86.77	150.1	45.98	96.61	155.5
17	38.71	86.30	149.9	39.13	86.77	150.1	45.98	96.61	155.5
Leissa [3]	38.71 (31)	86.30 (36)	149.9 (42)	39.13 (40)	86.77 (40)	150.1 (43)	45.97 (43)	96.61 (46)	155.5 (47)

Table 4  
Comparison of the DQ non-dimensional critical buckling loads  $N_{cr}^* = N_{cr}b^2/D$  from Timoshenko and the exact method for  $\alpha = 0$

	a/b							
	0.4 (m = 1)	0.5 (m = 1)	0.6 (m = 1)	0.7 (m = 1)	0.8 (m = 1)	0.9 (m = 1)	1.0 (m = 2)	
DQM (N = 17)	93.247	75.910	69.632	69.095	72.084	77.545	75.910	
Timoshenko [2]	93.2	75.9	69.6	69.1	71.9	77.3	75.9	
Power series method [3]	93.247	75.910	69.632	69.095	72.084	77.545	75.910	

independent of the plate dimensions and material constants. Table 1 lists first five non-dimensional frequencies  $\lambda(m = 1)$  of the plate. Symbols  $m$  and  $n$  denote the number of half-waves in the  $x$ - and  $y$ -direction as were used in Ref. [3]. Exact solutions as well as data by power series method [3] are also included for comparisons. As can be seen the convergence rate of DQ method is excellent. With  $N = 17$ , the DQ results are accurate to six significant figures for the first four modes and for four significant figures for the fifth mode. With  $N = 20$ , the DQ results are all accurate to six significant figures. The numbers in parenthesis after Leissa’s data are total

Table 5

Comparison of the DQ non-dimensional critical buckling loads  $N_{cr}^* = N_{cr}b^2/D$  from the power series and energy methods for  $\alpha = 1$

	<i>a/b</i>												
	0.4 ( <i>m</i> = 1)	0.5 ( <i>m</i> = 1)	0.6 ( <i>m</i> = 1)	0.64 ( <i>m</i> = 1)	0.65 ( <i>m</i> = 1)	0.66 ( <i>m</i> = 1)	0.67 ( <i>m</i> = 1)	0.7 ( <i>m</i> = 1)	0.8 ( <i>m</i> = 1)	0.9 ( <i>m</i> = 1)	1.0 ( <i>m</i> = 2)	1.2 ( <i>m</i> = 2)	1.4 ( <i>m</i> = 2)
DQM ( <i>N</i> = 17)	174.4	145.2	134.8	133.7	133.7	133.7	133.8	134.6	141.0	152.0	145.2	134.8	134.6
Energy method [3]	175	145	135	133.9	133.8	133.9	134.0	134.7	141.0	152.1	145	135	135
Series method [3]	174.4	145.2	134.8	133.7	133.7	133.7	133.8	134.6	141.0	152.0	145.2	134.8	134.6

Table 6

Comparison of the DQ non-dimensional critical buckling loads  $N_{cr}^* = N_{cr}b^2/D$  from the power series and energy methods for  $\alpha = 2$

	<i>a/b</i>														
	0.3 ( <i>m</i> = 1)	0.35 ( <i>m</i> = 1)	0.4 ( <i>m</i> = 1)	0.45 ( <i>m</i> = 1)	0.47 ( <i>m</i> = 1)	0.48 ( <i>m</i> = 1)	0.5 ( <i>m</i> = 1)	0.6 ( <i>m</i> = 1)	0.7 ( <i>m</i> = 1)	0.7 ( <i>m</i> = 2)	0.8 ( <i>m</i> = 2)	1.0 ( <i>m</i> = 2)	1.2 ( <i>m</i> = 3)	1.5 ( <i>m</i> = 3)	2.0 ( <i>m</i> = 4)
DQM ( <i>N</i> = 17)	464.4	422.5	400.4	391.3	390.5	390.5	391.5	411.8	451.6	422.5	400.4	391.5	400.4	391.5	391.5
Energy method [3]	467	424	402	392	390.9	391.1	382.2	412.2	452	424	402	392	402	392	382
Series method [3]	464.5	422.5	400.4	391.3	390.5	390.5	391.5	411.8	451.6	422.5	400.4	391.5	400.4	391.5	391.5

Table 7

Non-dimensional frequencies  $\lambda = \omega a^2 \sqrt{\rho h/D}$  of an SS-C-SS-C rectangular plate for  $\alpha = 0$  (*N* = 17)

<i>a/b</i>	$N_0/N_{cr}$	<i>n</i>	<i>m</i> = 1	<i>m</i> = 2	<i>m</i> = 3
0.5	0.0	1	13.69	42.59	91.70
		2	23.65	51.67	100.3
	0.5	1	9.677	37.93	86.99
		2	21.58	47.91	95.97
	0.8	1	6.120	34.85	84.03
		2	20.23	45.51	93.30
0.95	1	3.060	33.19	82.51	
	2	19.52	44.25	91.94	
1.0	1.0	1	0.00 (0)	32.63	82.00
		2	19.28	43.83	91.48
	0.0	1	28.95	54.74	102.2
		2	69.33	94.59	140.2
	0.5	1	21.53	38.71	84.12
		2	66.57	86.30	127.6
	0.8	1	15.45	24.48 (24.28)	71.09
		2	64.86	80.93	119.4
	0.95	1	11.24	12.24	63.58
		2	63.99	78.10	115.1
1.0	1	9.431	0.00 (0)	60.87	
	2	63.69	77.13	113.6	
2.0	0.0	1	95.26	115.8	156.4
		2	254.1	277.3	318.1
	0.5	1	87.85 (87.84)	89.32	110.6
		2	251.5	267.3	298.3
	0.8	1	83.08	68.69 (68.68)	69.93 (69.92)
		2	249.8	261.2	285.7
	0.95	1	80.59	55.57	34.96 (34.95)
		2	249.0	258.0	279.2
	1.0	1	79.74	50.45 (50.44)	0.00 (0)
		2	248.7	257.0	277.0

Table 8

Non-dimensional frequencies  $\lambda = \omega a^2 \sqrt{\rho h/D}$  of an SS-C-SS-C rectangular plate for  $\alpha = 1$  ( $N = 17$ )

$a/b$	$N_0/N_{cr}$	$n$	$m = 1$	$m = 2$	$m = 3$
0.5	0.0	1	13.69	42.59	91.70
		2	23.65	51.67	100.3
	0.5	1	9.781	37.94	86.95 (87.62)
		2	21.69	48.15	96.24 (92.46)
	0.8	1	6.224 (6.225)	34.65	83.73 (83.40)
		2	20.45	45.96	93.81 (94.82)
	0.95	1	3.121 (3.123)	32.83	82.01 (82.04)
		2	19.81	44.84 (44.83)	92.58 (90.42)
	1.0	1	0.00 (0)	32.19	82.41 (82.21)
		2	19.59	44.46	92.17 (87.81)
1.0	0.0	1	28.95	54.74	102.2
		2	69.33	94.59	140.2
	0.5	1	21.84	39.13	84.32
		2	66.70	86.77	128.4
	0.8	1	16.05	24.90	70.72
		2	65.09	81.81	120.9
	0.95	1	12.12	12.49	62.60
		2	64.27	79.25	117.0
	1.0	1	10.49	0.00 (0)	59.61
		2	64.00	78.37	115.7
2.0	0.0	1	95.26	115.8	156.4
		2	254.1	277.3	318.1
	0.5	1	88.04	89.94	111.3
		2	251.5 (251.3)	267.7	299.0
	0.8	1	83.40	69.70 (68.70)	70.69 (70.68)
		2	250.0	261.7	287.0
	0.95	1	80.97	56.85	35.42 (35.39)
		2	249.2	258.7	280.9
	1.0	1	80.14	51.85 (51.84)	0.00 (0)
		2	248.9	257.7	278.9

number of polynomial terms used in the power-series method to obtain the solutions accurate to four significant figures. It is pointed out by Leissa and Kang [3] that the convergence of the power-series method is not monotonic, but oscillating about the exact values as the total number of terms is increased, rather than approaching them from one direction.

Consider next the buckling of loaded SS-C-SS-C rectangular plates with various aspect ratios. Table 2 lists the non-dimensional critical buckling loads  $N_{cr}^*$  for  $\alpha = 0, 1, 2$ . Each loading case, three aspect ratios are considered. Leissa’s data [3] are also included for comparisons. As can be seen the convergence rate of DQ method is again excellent. With  $N = 13$ , the DQ results are accurate to four significant figures. The numbers in parenthesis after Leissa’s data are again the total number of polynomial terms used in the power-series method to obtain the same accurate solutions. If 53 terms are used, the power-series method yields more accurate buckling loads for  $\alpha = 0$  and  $a/b = 0.4, 0.5, 0.7, 93.2472, 75.9099, \text{ and } 69.0952$ , respectively. With  $N = 15$ , the DQ method can also yield the same accurate buckling loads to six significant figures.

Consider last the free vibration of a loaded SS-C-SS-C square plate under one-half of the critical buckling value ( $N_0/N_{cr} = 0.5$ ). Table 3 exhibits the convergence of the first three frequencies of the plate under three loading conditions ( $\alpha = 0, 1, 2$ ) for modes having two half-waves in the  $x$ -direction ( $m = 2$ ). Leissa’s data [3] are also included for comparisons. Again the convergence rate of DQ method is excellent. With  $N = 14$ , the DQ results are accurate to four significant figures. It is seen that more terms (numbers in parenthesis after Leissa’s data) of the series are needed for accurate results as the complexity of the mode shape increases.

The numerical results from the DQ approach, presented in the next sections, were obtained by taking  $N = 17$  to compare with accurate data obtained by the power-series method, although even smaller number of



Table 9

Non-dimensional frequencies  $\lambda = \omega a^2 \sqrt{\rho h/D}$  of an SS-C-SS-C rectangular plate for  $\alpha = 2$  ( $N = 17$ )

$a/b$	$N_0/N_{cr}$	$n$	$m = 1$	$m = 2$	$m = 3$	$m = 4$
0.5	0.0	1	13.69	42.59	91.70	160.7
		2	23.65	51.67	100.3	169.0
	0.5	1	11.49	37.93	86.14	154.7 (156.2)
		2	24.15	52.63	101.1	158.7 (161.0)
	0.8	1	7.684 (7.685)	31.74	79.57	147.8
		2	24.67	52.84	100.7	175.7 (172.1)
	0.95	1	3.926	27.64 (27.65)	75.66	144.0 (144.3)
		2	24.91	52.66	100.1	167.9 (163.4)
	1.0	1	0.00 (0)	26.08	74.26 (74.25)	142.7 (143.0)
		2	24.98	52.57 (52.55)	99.80 (99.58)	159.8 (160.8)
1.0	0.0	1	28.95	54.74	102.2	170.3
		2	69.33	94.59	140.2	206.7
	0.5	1	27.47	45.98 (45.97)	87.22	151.7
		2	69.65	96.61	143.6	210.5 (210.4)
	0.8	1	25.07	30.74	64.62	127.0
		2	70.11	98.68	145.7 (146.0)	211.4 (211.3)
	0.95	1	23.37	15.70	46.98 (46.96)	110.6
		2	70.41	99.63	146.0 (147.3)	210.7 (210.6)
	1.0	1	22.71	0.00 (0)	39.00	104.3
		2	70.51	99.92	146.1 (147.9)	210.3 (210.4)
2.0	0.0	1	95.26	115.8	156.4	219.0
		2	254.1	277.3	318.1	378.3
	0.5	1	94.76	109.9	137.3	183.9
		2	254.2	278.6	322.4	186.4
	0.8	1	93.98	100.3	104.5	123.0
		2	254.4	280.5	327.7	394.7
	0.9	1	93.64	95.90	87.80	88.21
		2	254.5 (254.4)	281.2	329.7	397.3
	0.95	1	93.46	93.47	77.50	62.82
		2	254.5	281.6	330.7	398.5
1.0	1	93.26	90.85	65.16	0.00 (0)	
	2	254.6	282.1	331.7	399.7	

grid points will yield similar accurate results. Leissa's data are obtained by using typically 70 terms or even 120 terms for  $a/b = 0.5$  and  $m = 3, 4$  in Table 9.

#### 4. Numerical results and discussions

The same cases as in Ref. [3] are restudied by using the DQ method to show the efficiently DQ method as well as to confirm the first known exact solutions. Various buckling loads and frequencies are listed in Tables 4–9. It should be pointed out that, however, one cannot know exactly the corresponding mode number of the frequency obtained by DQ method without plotting the mode shape.

Table 4 compares the non-dimensional critical buckling loads  $N_{cr}^*$  for plates under uniform loading ( $\alpha = 0$ ). It can be seen that DQ results are exactly the same as the exact solutions obtained by power-series method [3]. As can be seen that in most cases the three-digit results obtained by Timoshenko [2] agree also with the exact results [3], except for  $a/b = 0.8, 0.9$ , where there are small disagreements.

Tables 5 and 6 show the non-dimensional critical buckling loads  $N_{cr}^*$  for the linearly varying loading ( $\alpha = 1$ ) and the pure in-plane bending moment ( $\alpha = 2$ ), respectively. Again, exact solutions in Ref. [3] are reproduced by DQ method with  $N = 17$ . The approximate solutions obtained by the energy method are cited from Ref. [3] for comparison. As can be seen the results obtained by the energy method seem to be typically quite accurate, but not exactly the same as compared with the exact solutions.

Tables 7–9 list non-dimensional free vibration frequencies  $\lambda$  for three loadings ( $\alpha = 0, 1, 2$ ), respectively. For comparisons, results are also given in each table for three aspect ratios ( $a/b = 0.5, 1, 2$ ) and several load intensities ( $N_0/N_{cr} = 0, 0.5, 0.8, 0.95$  and 1), where  $N_{cr}$  is the lowest buckling load for the same plate. For load case of  $\alpha = 0$ ,  $N_{cr} = 75.9099$  for  $a/b = 0.5, 1$  and 68.8070 for  $a/b = 2$ . Mode shapes shown in Fig. 2 can explain why the buckling loads for  $a/b = 0.5, 1$  are exactly the same. As can be seen clearly from Fig. 2 that  $m = n = 1$  for  $a/b = 0.5$ ; and  $m = 2, n = 1$  for  $a/b = 1$ . For load case of  $\alpha = 1$ ,  $N_{cr} = 145.2055$  for  $a/b = 0.5, 1$  and 133.7894 for  $a/b = 2$ . For load case  $\alpha = 2$ ,  $N_{cr} = 391.5456$  for all three aspect ratios. In each table, there is only one datum if the DQ result is exactly the same as the datum in Ref. [3] for the case considered. There are two data if the DQ result is slightly different from the datum in Ref. [3], the datum in parenthesis is the result obtained by the power-series method. As can be seen from these tables, exactly the same data as in Ref. [3] are reproduced by the DQ method for most cases. For some cases, only the fourth significant figure is slightly different. To verify that the frequency evaluated from DQ method corresponds to the same mode as that of Ref. [3], two mode shapes are plotted in Fig. 3 for the case of a square plate with  $\alpha = 1$  and  $N_0/N_{cr} = 0.8$ . It can be seen from Fig. 3(a) that  $m = 2, n = 1$  when  $\lambda = 24.90$  and from Fig. 3(b) that  $m = 2, n = 2$  when  $\lambda = 81.81$ . From Table 8, one can see that the numbers of half-waves in the  $x$ - and  $y$ -direction are exactly the same as in Ref. [3].

As is noted, however, there are small disagreements between the DQ data and the data obtained by power-series method for cases of  $\alpha = 1, a/b = 0.5, m = 3$  (see Table 8) and  $\alpha = 2, a/b = 0.5, m = 4$  (see Table 9),

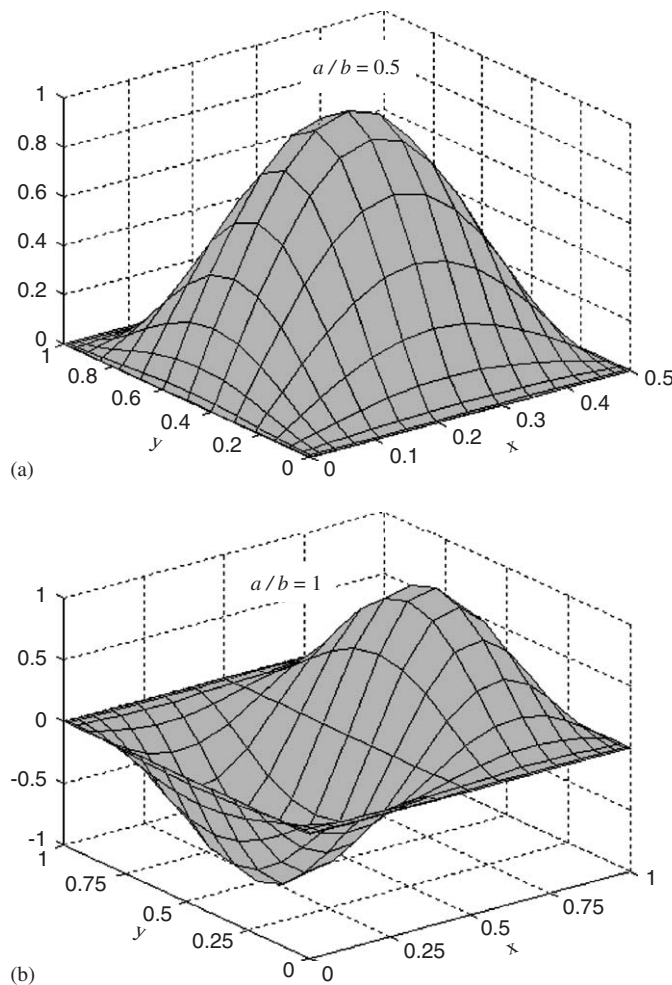


Fig. 2. Buckling modes of SS-C-SS-C rectangular plate under compressive load ( $\alpha = 0$ ).

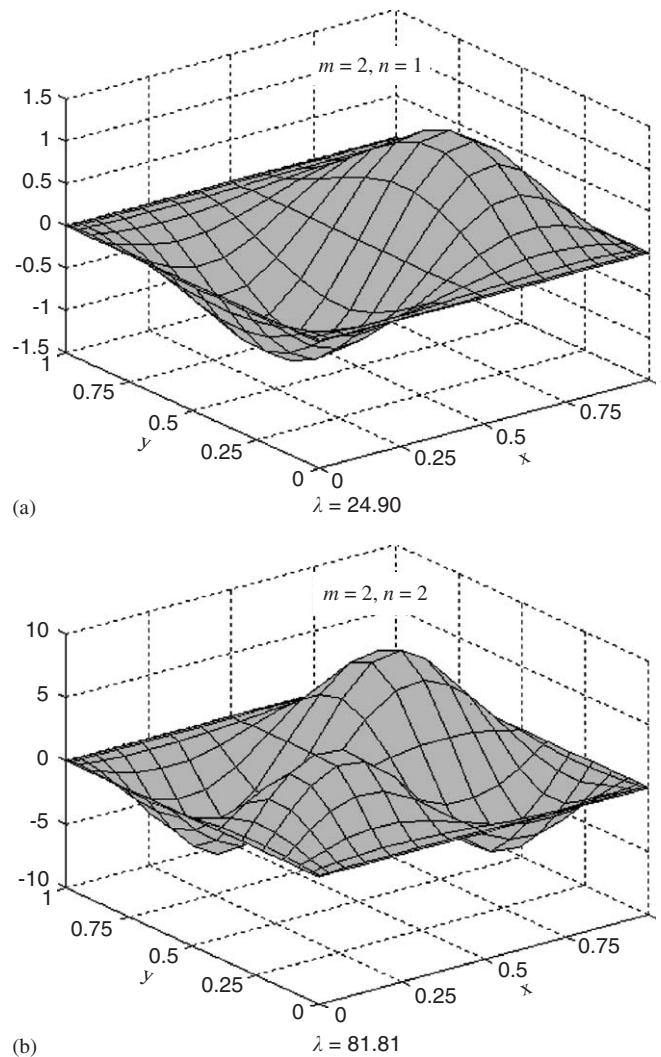


Fig. 3. Vibration modes of SS-C-SS-C rectangular plate under compressive load ( $a/b = 1$ ,  $\alpha = 1$ ,  $N_0/N_{cr} = 0.8$ ): (a)  $a/b = 0.5$ ; and (b)  $a/b = 1$ .

especially for the later case. For checking the correctness of DQ data, the grid number  $N$  is increased from 17 to 23 with step of 1, however, DQ results remain exactly the same as listed in Tables 8 and 9. It should be mentioned that the DQ data close to the data are listed in parenthesis. It is noticed that the convergence of the power series is slow and not monotonic, but oscillatory [3]. Most data in Tables 7 and 8 are obtained by using 70 terms of power series, but 120 terms of power series for data in Table 9 ( $a/b = 0.5$ ,  $m = 4$ ). Therefore, the slow and oscillatory convergence might cause the slight difference between the DQ results and data by power-series method.

## 5. Conclusions

In this paper, the DQ method is extended for the free vibration and buckling solutions of SS-C-SS-C thin plates subjected to linearly varying in-plane stresses. One of the boundary condition is built in during formulation of the weighting coefficients of higher-order derivatives to make DQ analysis even simpler. Then, differential quadrature equivalent is obtained to represent the governing differential equation and other boundary conditions. Convergence study shows that the rate of convergence is excellent. DQ method with grid

number of  $15 \times 15$  and non-uniform grid spacing can yield accurate results for all cases considered. Exactly the same accurate results as of Leissa and Kang [3] have been reproduced without any difficulty. It should be pointed out that the classical plate theory based on the Kirchhoff hypothesis is used in the analysis. However, the DQ method could be also extended for analysis of thick plates employing various shear deformable theories [11]. It is demonstrated that the DQ method could provide the benchmark for the development of other numerical techniques, since the DQ results are very accurate and almost the same as exact solutions for the case considered.

### Acknowledgment

The project is partially supported by the Aeronautical Science Foundation of China (04B52006).

### References

- [1] A.W. Leissa, The free vibration of rectangular plates, *Journal of Sound and Vibration* 31 (1973) 257–293.
- [2] S. Timoshenko, J. Gere, *Theory of Elastic Stability*, second ed., McGraw-Hill Book Company, Inc, New York, 1963.
- [3] A.W. Leissa, J.H. Kang, Exact solutions for vibration and buckling of an SS-C-SS-C rectangular plate loaded by linearly varying in-plane stresses, *International Journal of Mechanical Sciences* 44 (2002) 1925–1945.
- [4] C.W. Bert, K.K. Devarakonda, Buckling of rectangular plates subjected to nonlinearly distributed in-plane loading, *International J Solids and Structures* 40 (2003) 4097–4106.
- [5] A.K. Nayak, R.A. Shenoi, Assumed strain finite elements for buckling and vibration analysis of initially stressed damped composite sandwich plates, *Journal of Sandwich Structures and Materials* 7 (2005) 307–334.
- [6] A.K. Nayak, S.S.J. Moy, R.A. Shenoi, A higher order finite element theory for buckling and vibration analysis of initially stressed composite sandwich plates, *Journal of Sound and Vibration* 286 (2005) 763–780.
- [7] S.K. Sahu, P.K. Datta, Dynamic stability of curved panels with cutouts, *Journal of Sound and Vibration* 251 (2002) 683–696.
- [8] S.K. Sahu, P.K. Datta, Parametric instability of doubly curved panels subjected to non-uniform harmonic loading, *Journal of Sound and Vibration* 240 (2001) 117–129.
- [9] R. Bellman, J. Casti, Differential quadrature and long-term integration, *Journal of Mathematical Analysis and Applications* 34 (1971) 235–238.
- [10] C.W. Bert, S.K. Jang, A.G. Striz, Two new approximate methods for analyzing free vibration of structural components, *AIAA Journal* 26 (1988) 612–618.
- [11] F.L. Liu, K.M. Liew, Static analysis of Reissner-Mindlin plates by differential quadrature element method, *ASME Journal of Applied Mechanics* 65 (1998) 705–710.
- [12] X. Wang, C.W. Bert, A.G. Striz, Differential quadrature analysis of deflection, buckling, and free vibration of beams and rectangular plates, *Computers and Structures* 48 (1993) 473–479.
- [13] X. Wang, Differential quadrature in the analysis of structural components, *Advances in Mechanics* 25 (1995) 232–240 (in Chinese).
- [14] C.W. Bert, M. Malik, Differential quadrature in computational mechanics: A review, *Applied Mechanics Review* 49 (1996) 1–27.
- [15] C. Shu, *Differential Quadrature and its Application in Engineering*, Springer, London, 2000.
- [16] X. Wang, C.W. Bert, A new approach in applying of differential quadrature to static and free vibrational analyses of beams and plates, *Journal of Sound and Vibration* 162 (1993) 566–572.
- [17] X. Wang, F. Liu, X. Wang, L. Gan, New approaches in application of differential quadrature method for fourth-order differential equations, *Communications in Numerical Methods in Engineering* 21 (2005) 61–71.